MOLECULAR AND CELLULAR BIOLOGY, Dec. 2005, p. 11035–11046 Vol. 25, No. 24
0270-7306/05/$08.00+0 doi:10.1128/MCB.25.24.11035–11046.2005

Deficiency in Expression of the Signaling Protein Sin/Efs Leads to T-Lymphocyte Activation and Mucosal Inflammation

Laura T. Donlin,†‡ Nichole M. Danzl,† Celestine Wanjalla, and Konstantina Alexandropoulos*

Department of Pharmacology, College of Physicians and Surgeons of Columbia University, New York, New York 10032

Received 25 April 2005/Returned for modification 3 June 2005/Accepted 30 September 2005

Our studies have concentrated on elucidating the role of the signaling protein Sin in T-lymphocyte function. We have previously shown that Sin overexpression inhibits T-lymphocyte development and activation. Here we show that Sin-deficient mice exhibit exaggerated immune responses characterized by enhanced cytokine secretion and T-cell-dependent antibody production. Excessive T-cell responses in young mice correlate with spontaneous development of inflammatory lesions in different organs of aged $Sin^{-/-}$ mice, particularly the small intestine. The intestinal inflammation is characterized by T- and B-cell infiltrates in the lamina propria, which correlate with crypt enlargement and marked villus expansion and/or damage. Similar to the human intestinal inflammatory disorder Crohn's disease (CD), and in contrast to most mouse models of mucosal inflammation, inflammatory lesions in the gastrointestinal tract of $Sin^{-/-}$ mice are restricted to the small bowel. Taken together, these results suggest that Sin regulates immune system and T-lymphocyte function and that immune system dysfunction in the absence of Sin may underlie the pathogenesis of tissue-specific inflammation and enteropathies such as CD.

Inflammatory diseases of the gastrointestinal (GI) tract frequently result from immune reactions to harmless antigens in food and the mucosal microenvironment. In humans, mucosal inflammation can develop in any portion of the gastrointestinal tract, including the duodenum and the proximal jejunum (celiac disease), the entire length of the small intestine (Crohn's disease), and the colon (ulcerative colitis) (13, 35, 39). Multiple animal models of mucosal inflammation, which have been developed by chemical, immunological, or genetic means, demonstrate that different types of immune imbalances can lead to loss of tolerance to foreign antigens and inflammation in the gut (6, 8, 16, 32, 39, 48). Despite their different etiologies, once established, these diseases share common features which in most cases involve excessive helper T-cell responses. Aberrant T-cell responses are mediated by $CD4^+$ effector T cells which constitute the major cell population that infiltrates mucosal tissues in all experimental animal models studied so far (27, 33, 39).

We are interested in the molecular mechanisms that govern the development and function of T lymphocytes. Our recent experiments have concentrated on elucidating the role of the adapter protein Sin (*S*rc *in*teracting protein) in these processes. Sin is highly expressed in the thymus and was isolated as a ligand for the Src homology 3 (SH3) domain of Src kinases such as Fyn, an important regulator of T-lymphocyte signaling (2, 3). Sin, also known as embryonal Fyn substrate (Efs), belongs to a small family of adapter molecules, the Cas proteins, which include the prototype member p130Cas and HEF1/CasL (31). As adapter molecules, all three members contain conserved modular domains and motifs capable of mediating multiple protein-protein interactions. The conserved features of the Cas proteins include (i) proline-rich sequences that show binding specificity for the Src, Fyn, and phospholipase C-γ SH3 domains; (ii) tyrosine-based motifs which, when phosphorylated, bind to different Src homology 2 (SH2) domains on other proteins (36); (iii) an N-terminal SH3 domain that is highly conserved among the three family members and has the potential to bind to phosphatases (10, 31); (iv) and a conserved C terminus which can mediate homo- or heterotypic interactions between the different family members (20). All three members of the Cas family are substrates for Src kinases, and Src kinase-mediated phosphorylation of these proteins is important for their adapter signaling properties (3).

In previous experiments, we generated transgenic mice and T-cell lines expressing Sin to gain insight into the function of this protein in T lymphocytes. We found that overexpression of Sin results in defective thymocyte development and interleukin-2 (IL-2) production by mature T cells, suggesting a negative role for Sin in T-lymphocyte function (11, 49). In this report, we show that mice deficient in Sin expression exhibit exaggerated immune responses. More importantly, we found that aged Sin heterozygous and homozygous mice develop inflammatory lesions in their small intestine in the form of infiltrating $CD4^+$ T cells and B cells in the lamina propria. The presence of infiltrates correlates with villus expansion and/or destruction. Inflammatory infiltrates were also found in the liver and kidney of Sin-deficient mice and to a lesser extent in the lung and skin. Our results support a role for Sin as an important regulator of T-lymphocyte function and suggest that Sin deficiency leads to aberrant T-cell-mediated immune responses and tissue-specific inflammation.

* Corresponding author. Mailing address: Department of Pharmacology, College of Physicians and Surgeons of Columbia University, New York, NY 10032. Phone: (212) 305-2705. Fax: (212) 305-8780. E-mail: ka141@columbia.edu.

† L.T.D. and N.M.D. made equal contributions to this work.

‡ Present address: Laboratory of Lymphocyte Signaling, The Rockefeller University, 1230 York Ave., New York, NY 10021.

MATERIALS AND METHODS

Mice. A bacterial artificial chromosome (BAC) mouse genomic library containing DNA derived from embryonic stem cells of strain 129/SvJ (Incyte Corp.) was screened for the Sin locus. Four BAC clones containing the Sin genomic

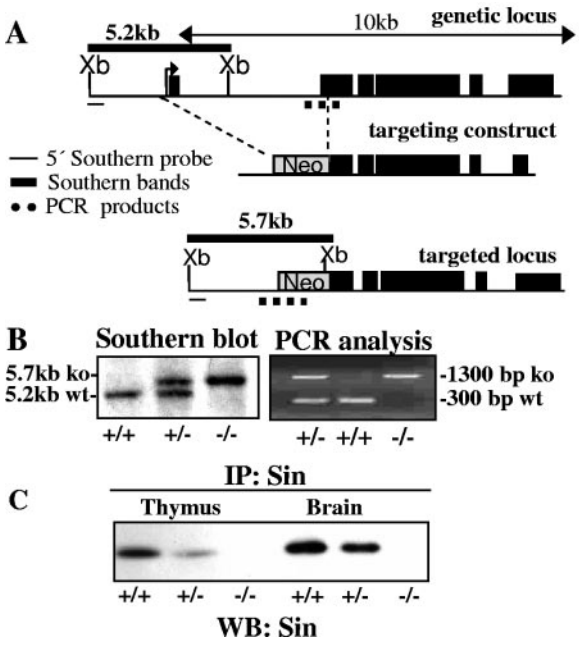

FIG. 1. Generation of Sin knockout mice. (A) To create a targeted disruption at the *sin* locus, we generated a targeting construct containing the neomycin resistance gene (Neo) under the transcriptional control of the phosphoglycerate kinase promoter. The 5′ short (1.5-kb) and 3′ long (4.0-kb) arms were obtained by PCR amplification using a BAC clone containing the Sin genomic locus. The deletion removes the first exon, the first intron, and part of the second exon, which disrupts the structure of the Sin-SH3 domain. (B) Genomic tail DNA from wild-type, heterozygous, and homozygous mice was digested with XbaI to reveal a ~5.2-kb wild-type (wt) fragment and a ~5.7-kb targeted fragment on Southern blots using a 5′ flanking probe (left panel). A PCR analysis of tail DNA from the same animals by using three primers is also shown (right panel). The primers amplify a 300-bp wild-type band and a 1.3-kb knockout (ko) band. (C) Cell lysates from whole thymus and brain from $Sin^{+/+}$, $Sin^{+/-}$, and $Sin^{-/-}$ mice were immunoprecipitated (IP) with Sin-specific antibodies, separated on sodium dodecyl sulfate-polyacrylamide gel electrophoresis, transferred onto nitrocellulose membranes, and probed with Sin antibody to reveal Sin protein levels. Protein bands were visualized by enhanced chemiluminescence. WB, Western blot.

locus were identified through hybridization to a cDNA probe spanning the entire coding region (amino acids 1 through 560; bp 1 through 1680) of Sin. The BAC clones were used to amplify sequences comprising the 5′ and 3′ arms of the targeting construct. The sequence for the primers was obtained from two contiguous sequences obtained from the ENSEMBL mouse genome database. The 5′- and 3′-arm PCR primers containing XhoI and KpnI sites were SinKO 5′-arm forward primer (GTCCATCTCGAGCCTGCAAAGTCAGCGTGCTCAAAC CGC), SinKO 5′-arm reverse primer (TACCTACTCGAGGGCTCTGTTTCG CTGACTTCAAGCGATG); SinKO 3′-arm forward primer (TAGCTAGGT ACCCAGGAACTGTCCTTCCGCCGAGGGGATGTT), SinKO 3′-arm reverse primer (GTCCATGGTACCGAGTAGGGTGGTAAAGCGTAGGGC CTG). The 5′ arm of the targeting sequence was cloned in an XhoI site, while the 3′ arm was cloned in a KpnI site. The targeting construct was electroporated into embryonic stem cells, and after antibiotic selection, four targeted clones were isolated. One of these clones was injected into blastocysts, which were then surgically implanted into recipient Swiss Webster mice. Male chimeric mice were then bred to C57BL/6J and 129/Sv females to establish mixed (C57BL/6J × 129/SvJ) as well as pure (129/SvJ) strains of mice. Germ line transmission of the targeted Sin locus was confirmed by analyzing tail DNA through PCR and Southern blot analysis. Animals were bred and maintained in a Columbia University animal facility under specific-pathogen-free (SPF) conditions and Institutional Animal Care and Use Committee guidelines. Animals in a C57BL/6J × 129/SvJ background as well as a 129/SvJ background were used in this study with similar results.

PCR and Southern blot analysis. The long-template PCR kit (Roche) was used for PCR genotyping. Two 5′ primers for the Sin wild-type locus (GAGGAG GAGTGTGCCCTCCATGACGCTGGCAGG) and the targeted locus (ATGGGA TCGGCCATTGAACAAGATGGATTG) were used for amplification. The 3′ primer for both loci was GGGACATGATGAGCCAGGCTGGGTGGGAGA TGC. For Southern blot analysis, 5 μg of purified tail DNA was loaded on a 0.8% Tris-borate-EDTA agarose gel and run overnight at 30 V. The DNA in the gel was then depurinated in 0.25 N HCl, and DNA was transferred onto a nylon membrane (Nytran SPC; Schleicher & Schuell) overnight by capillary action in transfer buffer (0.4 N NaOH, 1 M NaCl). Posttransfer, the membrane was soaked in 2 × SSC (1× SSC is 0.15 M NaCl plus 0.015 M sodium citrate), dried, and UV cross-linked. Hybridization was carried out in Ultrahyb buffer (Ambion, Inc.) with 0.5×10^6 cpm/ml of radiolabeled probe.

Flow cytometry analysis. A total of 10^6 freshly isolated thymocytes, splenocytes, or lymph node cells from 6- to 8-week-old mice were incubated with the specified antibodies and stained in MACS buffer (2 mM EDTA, 0.03% NaN_3, 1% bovine serum albumin, 1× phosphate-buffered saline [PBS]) for 15 min on ice. Cells were spun down and washed three times with MACS buffer, fixed in BD Cytofix buffer (BD Pharmingen), and analyzed by flow cytometry using a FACSCalibur and CELLQUEST software (BD Biosciences). Anti-CD4-allophycocyanin (APC)-, anti-CD8-peridinin chlorophyll *a* protein (PerCP)-, anti-CD3-fluorescein isothiocyanate (FITC)-, anti-CD69-FITC-, anti-CD5-FITC-, anti-T-cell receptor β (TCR-β)-FITC-, anti-CD62L-FITC-, anti-CD44-PE-, and anti-CD45-R(B220)-APC-conjugated antibodies were purchased from BD Pharmingen.

Immunoprecipitations and Western blots. These assays were performed as previously described (2). Mouse monoclonal antibody against Sin was obtained from BD Transduction Laboratories.

T-cell purification and proliferation/cytokine assays. Splenic $CD4^+$ T cells were purified by using the Dynabead/DETACHaBEAD mouse $CD4^+$ system (DYNAL Biotech). This protocol routinely yielded $CD4^+$ T-cell populations that were >95% pure, determined by staining cells with anti-CD4 antibody and analyzing them by fluorescence-activated cell sorting (FACS). A total of 1×10^5 to 2×10^5 $CD4^+$ T cells per well of a 96-well plate were plated. Cells were left untreated or induced with plate-bound mouse anti-CD3ε, anti-CD3ε/CD28 antibodies, or phorbol myristate acetate (PMA) and ionomycin. To measure proliferative responses, 48 h after stimulation, cells were labeled overnight with 1 μCi [^{3}H]thymidine, and T-cell proliferation was determined by levels of [^{3}H]thymidine incorporation on a scintillation counter. To measure cytokine secretion, culture supernatants were collected at 24 (IL-2) or 48 h and assayed for cytokine secretion by using a Luminex cytokine/chemokine sixplex bead and enzyme-linked immunosorbent assay (ELISA) kits according to the manufacturer's protocol (Biosource).

ELISAs. To measure T-cell-dependent responses, mice were immunized with 100 μg NP-keyhole limpet hemocyanin (KLH) by intraperitoneal injection, and blood was collected on day 14 after injection. NP_{12}-bovine serum albumin-coated plates were incubated with serially diluted sera for 2 h at 37°C. After washing the plates the levels of NP-specific immunoglobulin (Ig)-isotype production in response to immunization were determined using an isotype-specific ELISA kit (Southern Biotech) containing anti-isotype-specific secondary antibodies and anti-IgH-IgL for total Ig detection according to manufacturer's protocol and as previously described (41, 43). Titration curves of the different dilutions were constructed by measuring the absorbance of alkaline phosphatase color reactions at 405 nm. Antibody presence was expressed as absorbance at 405 nm from the 1:300 (or 1:3,600 in the case of IgG1) dilution, which was within the linear part of the titration curve. For statistical analysis, Student's *t* test was used to calculate statistical significance for differences in measurements between two different groups. A P value of <0.05 was considered statistically significant. Serum Ig levels from unimmunized aged mice were determined using the same isotype-specific ELISA kit (Southern Biotech).

Histological analysis. Various organs removed from aged mice were fixed in 10% buffered formalin and embedded in paraffin. Sections were stained with hematoxylin and eosin (H&E) and examined under a microscope with the help of a pathologist. The severity of the lesions was determined by light microscopy and staining of small intestine sections with anti-CD3 and anti-kappa light chain antibodies to determine the extent of infiltration and expansion/damage of villi. To classify severity of mucosal lesions, three distinct stages of villous damage relating to the extent of epithelium and lamina propria destruction were taken into consideration (mild, moderate, and severe).

Immunohistochemistry. Immunohistological staining was performed on paraffin-embedded or frozen sections of various organs by using alkaline phospha-

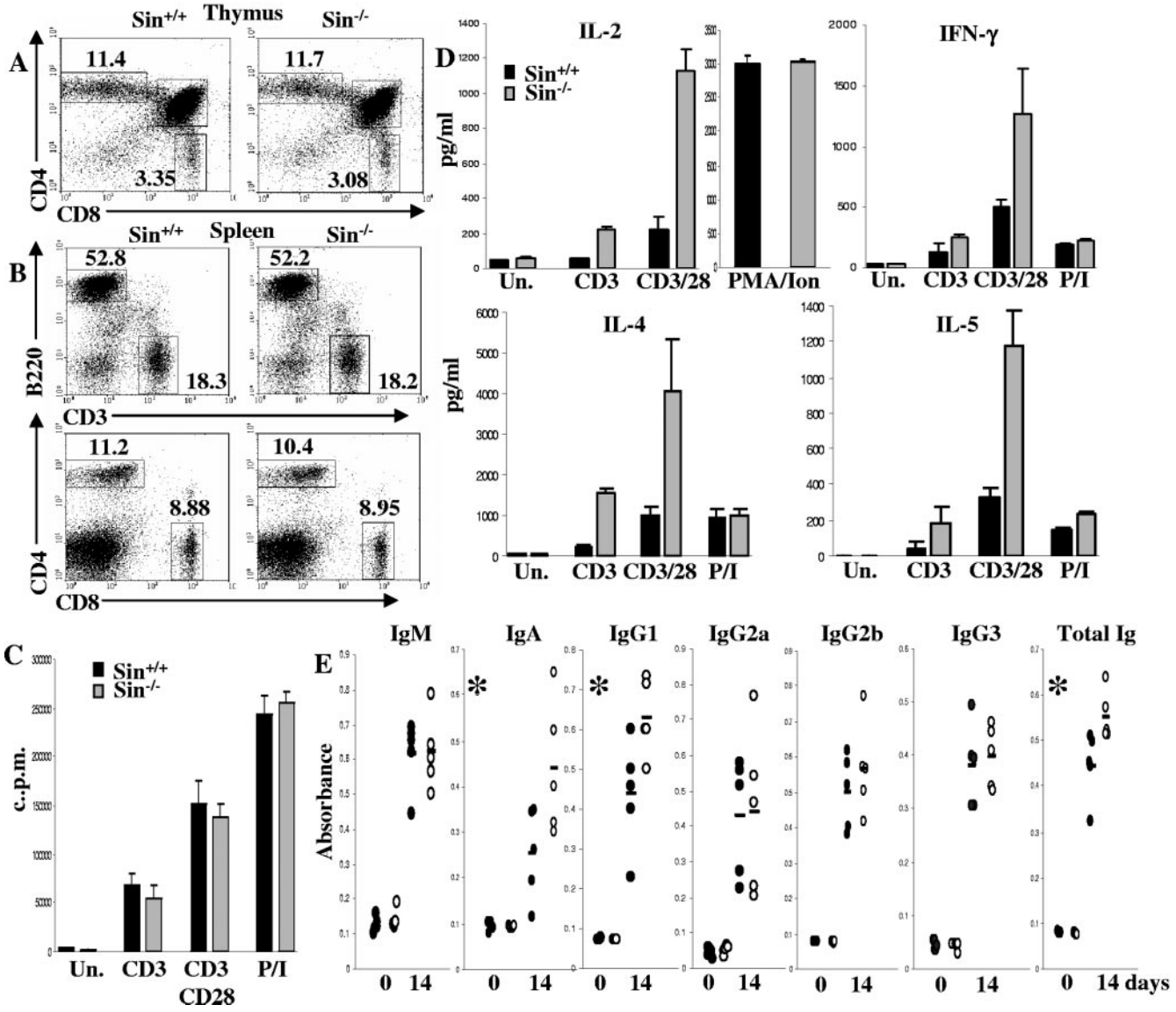

FIG. 2. Sin-deficient animals exhibit normal thymocyte development but increased T-cell responses. (A) A total of 1×10^6 thymocytes from wild-type and $Sin^{-/-}$ animals were stained with anti-CD4-APC and -CD8-PerCP antibodies to reveal different thymocyte populations (dot plots). (B) Total splenocytes (1×10^6) from normal and $Sin^{-/-}$ mice were stained with anti-B220-APC and anti-CD3-FITC antibodies or with anti-CD4-APC/CD8-PerCP and analyzed by FACS. Numbers represent percentage of cells within the boxed areas. At least five mice for each wild-type and Sin knockout phenotype were analyzed for the experiments described for panels A and B. (C) A total of 1×10^5 T cells were plated on a 96-well plate, and cells were left untreated or induced with plate-bound mouse anti-CD3ε (0.05 μg/ml), anti-CD3ε (0.5 μg/ml) and -CD28 (5 μg/ml) antibodies, or PMA (50 ng/ml) and ionomycin (500 ng/ml). Proliferation rates were determined at ~60 h after stimulation by measuring thymidine incorporation. Bars represent means of triplicate samples ± standard deviations. Shown is one of three representative experiments. (D) $CD4^+$ T cells were stimulated with anti-CD3 and -CD3/CD28 or with PMA-ionomycin (P/I) as described for panel C for 24 (IL-2) or 48 h. Culture supernatants were removed and cytokine concentrations were determined as described in Materials and Methods. The assay was performed in triplicates and bars represent means ± standard deviations. Six mice of each genotype were analyzed. Un., untreated. (E) Antibody production in response to NP-KLH immunization was measured using serum from mice at day 0 and 14 days after immunization and ELISAs. Lines represent the average antibody levels from five animals for each genotype. Student's *t* test was used to calculate statistical significance for differences in measurements between two Ig isotypes (IgG1, IgA, and total Ig) in wild-type and $Sin^{-/-}$ mice. ∗, a *P* value of <0.05, which was considered statistically significant.

tase (AP)-, horseradish peroxidase (HRP)-, or fluorophore-conjugated secondary antibodies. For staining paraffin-embedded sections, slides were deparaffinized with xylene, washed with ethanol, and after antigen retrieval (boiling for 15 min, in 1 mM EDTA, pH 7.5, followed by methanol washes), slides were blocked in 5% dry milk in TBST (0.05 M Tris, pH 7.5, 0.15 M NaCl, 0.01% Tween 20) and incubated with primary antibodies (anti-CD3 [Dako], anti-kappa light chain [Cortex]) overnight at room temperature (RT) in a humidified chamber. Slides were then washed with TBST and incubated with AP- or HRP-conjugated secondary antibodies for 30 min at RT. After washing in TBST specific staining was visualized by incubating slides in developing solutions nitroblue tetrazolium/BCIP (5-bromo-4-chloro-3-indolylphosphate) (AP; Roche) or aminoethylcarbacole (HRP; Sigma). For staining frozen sections, slides were fixed in 4% paraformaldehyde in PBS (pH 7.4) for 20 min, washed with PBS, and permeabilized/blocked with permeabilization buffer (RPMI medium, 0.05% saponin, 10 mM glycine, 5%

TABLE 1. Normal hematopoietic cell populations in $Sin^{+/+}$ and $Sin^{-/-}$ mice[a]

Parameter for cells	Value for:		No. of samples
	$Sin^{+/+}$	$Sin^{-/-}$	
Thymus			
Total cell no. (10^6)	103.0 ± 17.2	108.0 ± 24.5	8
% Cells			
$CD4^+$ $CD8^+$	78.1 ± 6.1	79.3 ± 4.3	8
$CD4^+$ $CD8^-$	10.3 ± 2.2	12.0 ± 2.8	8
$CD4^-$ $CD8^+$	2.5 ± 0.4	3.0 ± 0.7	8
Spleen			
Total cell no. (10^6)	56.0 ± 4.5	56.8 ± 9.0	6
% Cells			
$CD4^+$ $CD8^-$	19.5 ± 6.9	19.3 ± 5.4	5
$CD4^-$ $CD8^+$	11.7 ± 2.5	10.3 ± 0.8	5
$CD3^+$	40.2 ± 9.6	36.0 ± 8.7	5
$B220^+$	48.6 ± 8.1	48.6 ± 6.0	5
$CD4^+$ $CD25^+$	1.9 ± 0.1	2.3 ± 0.8	4
$CD4^+$ $CD62L^{hi}$ $CD44^{lo}$	57.6 ± 5.3	57.2 ± 7.5	5
Lymph node			
Total cell no. (10^6)	23.4 ± 2.8	20.2 ± 5.2	5
% Cells			
$CD4^+$ $CD8^-$	45.6 ± 5.0	52.7 ± 4.2	5
$CD4^-$ $CD8^+$	25.2 ± 4.3	25.6 ± 3.1	5
$CD3^+$	67.0 ± 10.0	75.7 ± 5.1	5
$B220^+$	21.6 ± 3.2	16.0 ± 3.7	5

[a] Numbers represent mean percentage values ± standard deviations. Total thymocytes, splenocytes, and lymph node cells from littermate 6 to 8-week-old wild-type and Sin-deficient mice were counted, and cell percentages were determined by FACS analysis using anti-CD4, -CD8, -CD3, -CD25, -CD62L, -CD44, and -B220 antibodies.

normal donkey serum). After washing, the slides were incubated with primary antibodies at a 1:100 dilution (anti-CD4, -CD8, or -CD25-FITC [BD Pharmingen], or anti-F480 [Serotech]) and incubated for 30 min at RT. After a washing, slides were incubated with anti-rabbit antibody–AlexaFluor 488 (Molecular Probes) or anti-rat antibody–rhodamine (Jackson ImmunoResearch) at a 1:400 dilution for 30 min at RT, and specific staining was visualized by fluorescent microscopy using a Nikon eclipse E600 microscope.

RESULTS

Generation of Sin-deficient mice. To explore the physiological role of Sin in T-lymphocyte function we generated mice deficient in Sin expression by homologous-recombination-mediated gene targeting. The targeting strategy involved insertion of a neomycin resistance cassette into the Sin locus, replacing a 4.3-kb fragment containing the first exon, the first intron, and a short portion of the second exon (Fig. 1A). The deletion was confirmed by analyzing tail DNA by Southern blots using a 5′ probe outside the targeted region and by PCR (Fig. 1B, left and right panels, respectively). The absence of Sin protein expression in knockout animals was confirmed in cell extracts from the brain and thymus, which normally express high levels of Sin (Fig. 1C) (3).

Normal T- and B-cell development but enhanced effector immune responses in Sin-deficient mice. Sin homozygous mice develop normally and are born at normal Mendelian frequencies. To examine the role of Sin deficiency on T-cell maturation, thymocyte and splenic T-cell suspensions were analyzed by flow cytometry for expression of the CD4/CD8 coreceptors and maturation/activation markers (4, 5). The $CD4^+$ and $CD8^+$ T-cell percentages in the thymus (Fig. 2A) and the ratio of B cells to T cells (Fig. 2B, top panels), as well as the percentages of $CD4^+$ and $CD8^+$ T cells in the spleen of Sin-deficient mice, were normal compared to those of wild-type littermates (Fig. 2B, bottom panels). Total CD3, TCR-β, CD5, CD69, CD62L, CD44, and CD25 levels in thymocytes and splenic T cells from Sin knockout animals were similar to those in thymocytes and splenic T cells from wild-type controls (Table 1; data not shown). Development of B cells assayed by IgD/IgM, CD23/CD21, and B220/IgM antibody staining was normal in $Sin^{-/-}$ mice (data not shown).

We have previously shown that Sin overexpression inhibits T-cell activation and IL-2 production (11, 49). Therefore, we tested the effect of Sin deletion on T-cell proliferation and cytokine secretion in vitro. Purified $CD4^+$ T cells were stimulated with plate-bound antibodies against the TCR and the CD28 costimulatory receptor or PMA and ionomycin. Proliferation was subsequently assayed by thymidine incorporation, while culture supernatants were analyzed for cytokine concentrations. We found that whereas proliferation was normal (Fig. 2C), the cytokine responses of $Sin^{-/-}$ T cells were enhanced in response to TCR stimulation, shown by increased production of IL-2 (5-fold) as well as cytokines of the Th_1 (IFN-γ [2-fold]) and Th_2 (IL-4 and IL-5 [~4-fold]) T-cell lineages (Fig. 2D). In contrast, T cells stimulated with PMA-ionomycin, a nonphysiological stimulus that bypasses the TCR, behaved no different that wild-type controls (Fig. 2D).

To characterize the in vivo function of Sin-deficient T cells, we tested the T-cell-dependent antibody responses of normal and Sin-deficient mice. Mice were immunized with NP-KLH, and antibody levels in the sera of different mice were analyzed by ELISAs. In Sin-deficient mice, most NP-specific immunoglobulin isotype levels were similar to those of wild-type controls (Fig. 2E). However, significant increases were observed in the levels of IL-4- and transforming growth factor β/IL-5-dependent IgG1 and IgA isotypes, respectively (38), which correlated with the enhanced IL-4/IL-5 cytokine production by Sin-deficient T cells (Fig. 2D). A concomitant significant increase in total Ig levels was also observed in the sera of $Sin^{-/-}$ mice compared to controls (Fig. 2E). The basal levels of serum immunoglobulin isotypes before immunization were within the normal range in all animals tested (Fig. 2E). Taken together, these data suggest that endogenous Sin plays an inhibitory role in T-lymphocyte function which is consistent with our previous studies showing a negative effect of Sin overexpression in T cells.

Spontaneous enteropathy in aged Sin-deficient mice. Previous studies on adapter proteins expressed in T cells have shown that the deletion of negative regulators in most cases results in increased proliferative responses and development of spontaneous autoimmunity in older mice (9, 17, 23, 28, 30, 37, 42, 47). To address the effect of Sin deficiency on development of spontaneous autoimmunity or inflammation, histopathological analyses were performed in older mice ranging in age from 7 to 14 months. While inflammatory infiltrates were detected in H&E sections of several organs derived from $Sin^{-/-}$ mice (see Table 3 below), we found that one of the tissues most seriously and consistently affected was the small intestine (Fig. 3A). H&E-stained sections of the duodenum/proximal jejunum revealed crypt hyperplasia and marked lymphocytic infiltration

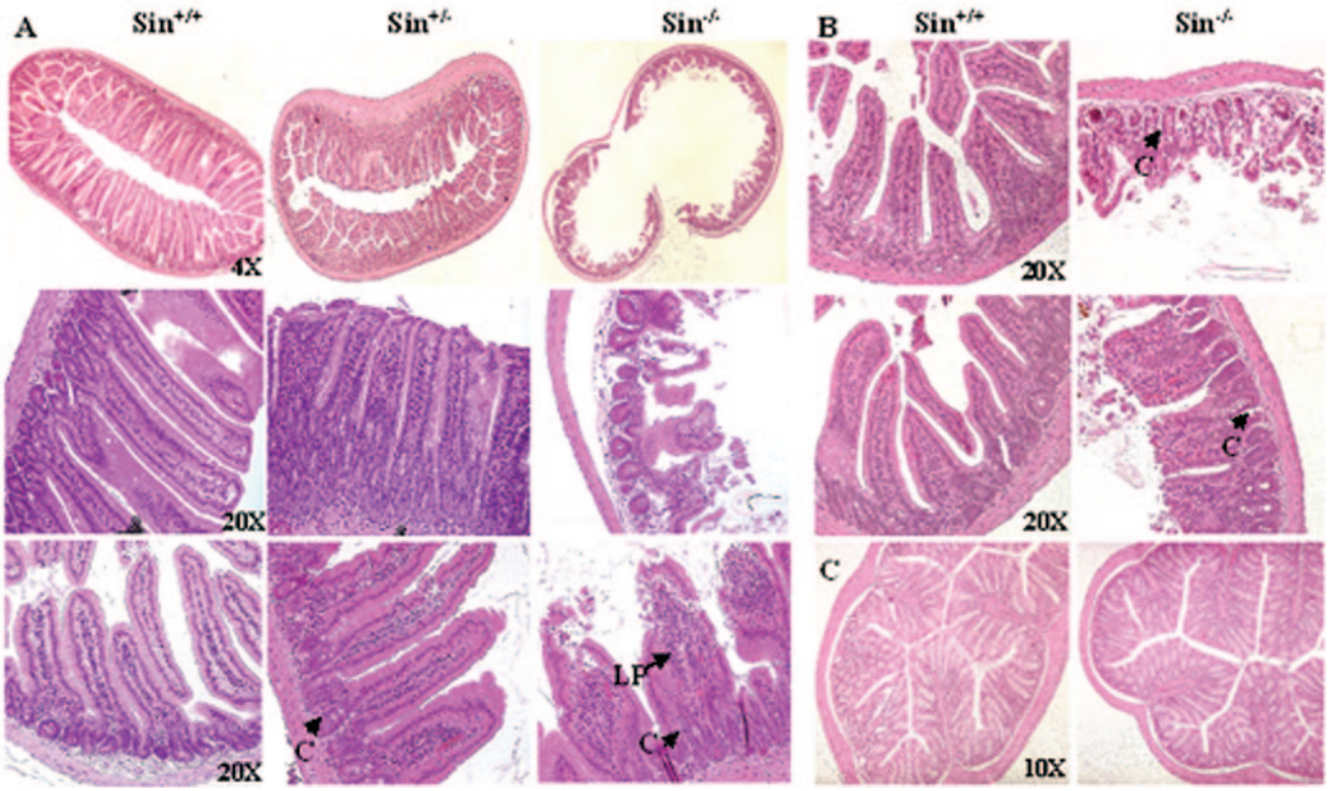

FIG. 3. Increased villus expansion/destruction and infiltration in the small intestines of $Sin^{+/-}$ and $Sin^{-/-}$ mice. (A) Paraffin-embedded sections of duodenum/proximal jejunum derived from 11-month-old littermate wild-type, heterozygous, and Sin knockout mice (two different animals of each genotype) were stained with H&E and visualized by light microscopy. Images in the top and middle panels were derived from the same animals, shown under two different magnifications. Arrows and arrowheads indicate the lamina propria (LP) and crypts (C). Paraffin-embedded sections of the ilea of two littermate wild-type and two $Sin^{-/-}$ animals (B), and the colons of $Sin^{+/+}$ and $Sin^{-/-}$ mice (one each) (C) were stained with H&E.

of the lamina propria, correlating with various degrees of damage in the intestinal mucosa of $Sin^{-/-}$ mice compared to intact wild-type controls (Fig. 3A, compare left and right panels). Interestingly, sections derived from heterozygous littermates exhibited an intermediate phenotype manifested as shortened, blunt villi, expanded laminae propriae, and enlarged crypts (Fig. 3A, middle panels).

The effects of Sin deficiency on villus expansion and damage were analyzed in multiple mice and classified according to their severity. While wild-type mice had normal mucosa, most heterozygote mice (6/8, 75%) had villi with expanded laminae propriae, of which a small percentage (~30%) also exhibited mild destruction at the tips of their villi. More dramatically, the majority (5/7, ~70%) of Sin-deficient mice exhibited marked infiltration of the lamina propria accompanied by moderate (3/5) or severe (2/5) villus destruction (Table 2; Fig. 3A, middle and bottom right panels, respectively). Similar effects were also observed in H&E sections derived from the ileum of Sin-deficient animals, ~60% of which exhibited inflammation and expansion of the lamina propria, crypt enlargement, and altered epithelial cell morphology or damage (Fig. 3B). In all but one case, inflammation in the duodenum/proximal jejunum coincided with inflammation in the ileum. In contrast, we found no evidence of inflammation in the colon of Sin-deficient animals (Fig. 3C).

Inflammatory infiltrates in the small intestine of Sin-deficient mice consist of T and plasma B cells. In experimental models of intestinal inflammation, villus expansion results from infiltration of the lamina propria and the intestinal epithelium by inflammatory cells, particularly lymphocytes (39, 40). To analyze the nature of the inflammatory infiltrates in the lamina propria and epithelium of Sin-deficient mice, serial small intestine sections derived from mice with extensive villus

TABLE 2. Presence and severity of inflammation in the small intestine of Sin-deficient mice[a]

Mouse type	No. of mice with indicated characteristic/total no. of mice				
	Expansion	Blunting	Villus damage		
			Mild	Moderate	Severe
$Sin^{+/+}$	1/6	0/6	0/6	0/6	0/6
$Sin^{+/-}$	6/8	3/8	2/8	0/8	0/8
$Sin^{-/-}$	5/7	1/7	0/7	3/7	2/7

[a] Blunting and severity of villus damage were determined by analyzing H&E-stained paraffin sections of the small intestine under a light microscope. Villus expansion was determined by increased presence of infiltrates determined by staining of small intestine paraffin sections with anti-CD3 and anti-kappa light chain antibodies. Littermate animals that were controlled for age and sex were used in these experiments. There was no gender bias in the development of inflammation as male and female mice were equally affected.

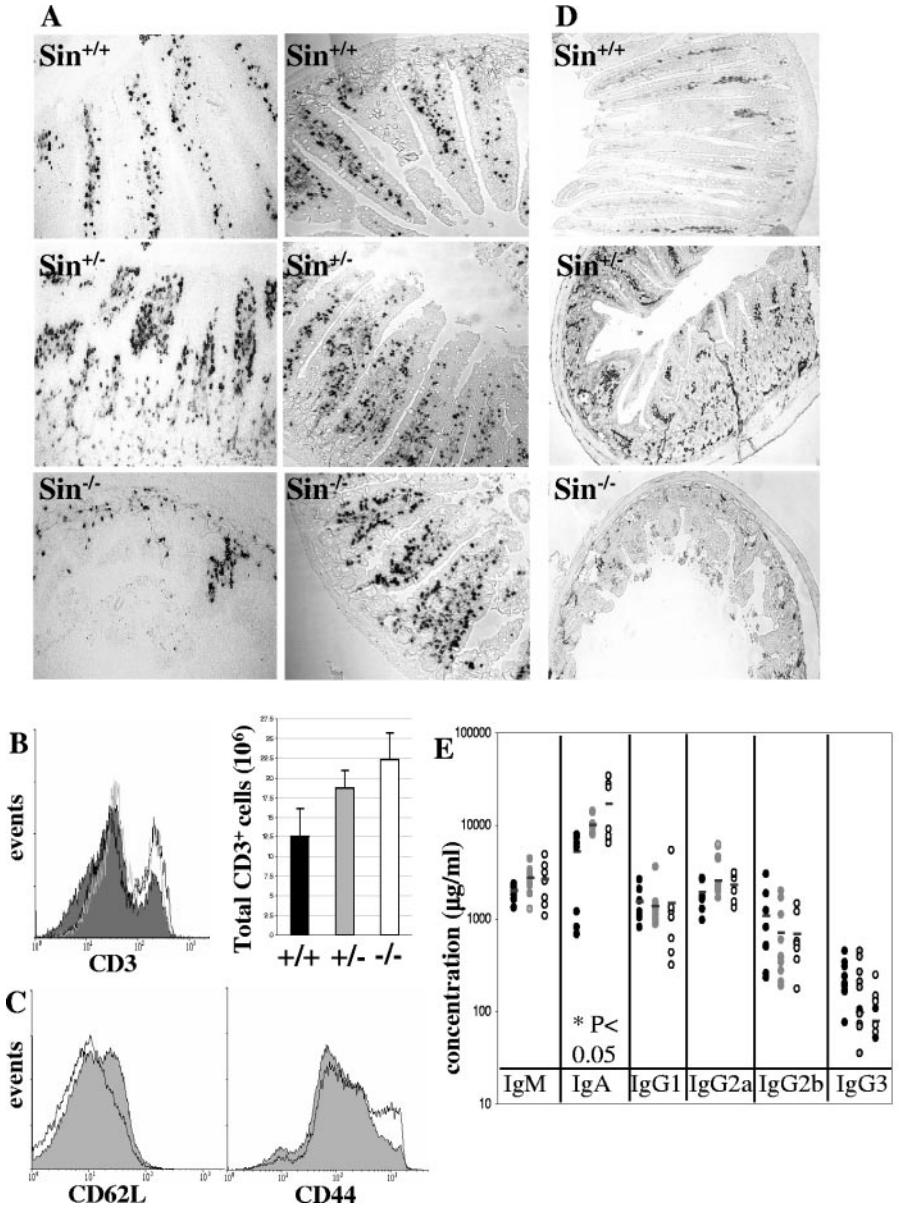

FIG. 4. Increased infiltration of the intestinal laminae propriae of $Sin^{+/-}$ and $Sin^{-/-}$ mice by $CD3^+$ T cells. (A) Serial sections from the small intestine of animals shown in Fig. 3A (middle panels) and a different set of littermate control, $Sin^{+/-}$, and $Sin^{-/-}$ mice with moderate villus destruction were stained with anti-CD3 antibody. (B) Total splenocytes (1×10^6) isolated from the same mice shown in panel A (left panels) were stained with anti-CD4, -CD8, and -CD3 antibodies, and total levels of CD3 (histogram) were determined by FACS. The filled curve represents $Sin^{+/+}$ mice; the black line, $Sin^{+/-}$; and the gray line, $Sin^{-/-}$ mice. Total numbers of splenic $CD3^+$ T cells from at least three mice for each genotype were determined by staining splenocytes with CD4/CD8/CD3 antibodies and flow cytometry (bar graph, means ± standard deviations). (C) Levels of CD62L CD44 expression of wild-type (filled curve) and $Sin^{-/-}$ mice (line) were determined by staining with specific antibodies and flow. Representative data ($n = 4$) are shown as histograms. (D) Serial paraffin-embedded sections from the same mice shown in panel A were stained with anti-kappa light chain antibodies to reveal the presence of plasma B cells. (E) Levels of immunoglobulin isotypes in the sera of aged, unimmunized animals were determined using an isotype-specific ELISA kit (Southern Biotech) according to manufacturer's protocol. Black circles represent wild-type animals; gray circles, heterozygous animals; and open circles, knockout animals. Lines represent the average antibody concentration from at least seven animals for each genotype. Student's *t* test revealed a significant ($P < 0.05$) threefold increase in IgA levels in $Sin^{-/-}$ mice.

destruction (shown in Fig. 3A) and an additional set of mice with moderate villus damage were stained with anti-CD3ε antibody to detect the presence of T cells. Immunostaining revealed increased presence of $CD3^+$ T cells in the lamina propria in sections derived from $Sin^{+/-}$ and $Sin^{-/-}$ mice compared to wild-type controls (Fig. 4A). The presence of $CD3^+$ T cells was less evident in the small intestine of $Sin^{-/-}$ mice with extensive villus damage, although dense staining was present in remnants of the villi (Fig. 4A, bottom left panel) and in mice with less extensive destruction (Fig. 4A, bottom right panel).

Consistent with the increased $CD3^+$ T-cell-specific staining in the laminae propriae of Sin-deficient mice, increased numbers of peripheral (splenic) $CD3^+$ T cells were observed in aged mice analyzed by anti-CD3 antibody staining and flow cytometry (Fig. 4B). Splenic $CD4^+$ T cells from Sin-deficient mice also exhibited increased levels of the surface marker CD44 with a concomitant decrease in CD62L expression, suggesting an activated, effector/memory T-cell phenotype (Fig. 4C). Serial sections of the same tissues used in Fig. 4A (left panels) were also stained with anti-kappa light chain antibody, which revealed increased presence of plasma B cells in a staining pattern similar to that obtained with anti-CD3 antibody (Fig. 4D). Serum concentrations of immunoglobulin isotypes were similar in aged unimmunized animals, with the exception of IgA, which showed a statistically significant threefold increase in Sin knockout animals (Fig. 4E).

Increased infiltration of the lamina propria by $CD4^+$ $CD25^+$ T cells in Sin-deficient mice. While $CD4^+$ T cells constitute the major infiltrating cell population in different mucosal inflammatory disease models (39), $CD8^+$ T cells are not essential for disease development, although they may contribute to the maintenance of inflammatory lesions (34). However, $CD8^+$ T-cell-mediated cytotoxicity has been implicated as the driving factor for the development of colitis in at least one experimental mouse model, the $TNF^{\Delta ARE}$ mice which exhibit enhanced production of tumor necrosis factor-α (18). To further characterize the nature of the infiltrates present in the small intestine of Sin-deficient mice, serial frozen sections of small intestine were stained with CD3/CD4, CD3/CD8, or CD4/$CD25^+$ antibodies and analyzed by fluorescent microscopy. Sin knockout mice exhibited marked infiltration of the lamina propria by $CD4^+$ T cells, which correlated with shortening and expansion of the villi (Fig. 5A, top right panel). The effect of Sin deficiency on infiltration of the lamina propria and intestinal epithelium by $CD8^+$ T cells was less dramatic but consistent, particularly in the case of Sin heterozygous mice which exhibited significant differences in the presence of intraepithelial (IE) $CD8^+$ T cells compared to controls (Fig. 5B). Costaining of the same sections with anti-CD3 and anti-CD4 or -CD8 antibodies and merging of the fluorescent images revealed that the infiltrates in the lamina propria consisted mostly of $CD3^+$ $CD4^+$ T cells, whereas $CD3^+$ $CD8^+$ cells were prominent in the intestinal epithelium (Fig. 5A and B, bottom right panels, and bar graphs in Fig. 5A).

As described for Fig. 2 above, we found that $Sin^{-/-}$ T cells exhibit enhanced immune responses suggesting an activated state for these cells. Activated $CD4^+$ T cells have been known to express on their surface markers such as CD69 and the IL-2 receptor CD25 in response to TCR stimulation. Thus, we tested whether the infiltrates we observe in $Sin^{+/-}$ and $Sin^{-/-}$ small intestine correlate with the presence of activated $CD4^+$ T cells in the lamina propria. Costaining cells with anti-CD4 and anti-CD25 antibodies and merging of the images revealed increased presence of $CD4^+$ $CD25^+$ T cells in the laminae propriae of Sin heterozygous and knockout mice with less severe villus destruction (Fig. 5C, bottom right panel).

Sin-deficient mice develop liver granulomas. In addition to the effects of Sin deficiency in the gut, inflammatory infiltrates were also found in the liver of ~70% (5/7) of Sin knockout animals. Inflammation in the liver consisted of infiltrates present around hepatic vessels and granulomas arising as multiple foci within the parenchyma (Fig. 6A). Granulomas in humans and mice arise as a result of diverse etiologies, are epithelioid in nature, and consist of both T cells and macrophages (21). Analysis of the cellular composition of liver sections with anti-CD3ε antibody staining revealed the presence of $CD3^+$ T-cell infiltrates in the liver of Sin knockout mice but not in wild-type controls (Fig. 6B). Staining of liver sections with the macrophage antigen F4/80 also revealed the presence of these cells in the granulomas (Fig. 6C). Liver granulomas coincided with the presence of infiltrates/damage in the small intestine in all cases examined suggesting a common link in the development of these inflammatory lesions. Inflammatory infiltrates were also found in the kidneys of most knockout animals that also developed intestinal and liver inflammation. Other tissues, such as the lung and skin, were less affected, and in some but not all cases, the lung inflammation occurred independently from that observed in the small intestine (Table 3).

DISCUSSION

In this report, we examined the role of the adapter molecule and signaling protein Sin in the function of the immune system, particularly T lymphocytes, by using mice deficient in Sin expression. We found that Sin deficiency led to exaggerated T-cell-mediated immune responses in young mice and T-cell-containing inflammatory lesions in aged animals. Specifically, Sin haploinsufficiency resulted in increased presence of inflammatory infiltrates in the small intestines of mice, whereas ablation of Sin expression led to marked T- and B-lymphocyte infiltration which coincided with destruction of the intestinal mucosa and increased levels of serum IgA, respectively. Taken together, these results suggest that endogenous Sin is a regulator of T-lymphocyte function such that the deletion of Sin leads to aberrant activation of T cells and development of T-cell-mediated inflammatory responses.

The inflammation in the Sin knockout mice appears in a specific subset of tissues, namely, the small intestine, liver, and kidney tissues, and to a lesser extent, lung and skin tissues. Based on our results, we propose that these effects are mediated by aberrant immune responses, particularly in the T-cell compartment, and are not due to a disturbance of the different organs as a result of Sin deficiency as most of the organs examined do not express the Sin protein (unpublished observations). This is particularly true in the case of the small intestine, in which, although we observe extensive epithelial cell damage, we have found no evidence of Sin expression in the intestinal epithelium.

Consistent with the concept that an aberrant immune response mediates inflammation in Sin-deficient mice, we found that $Sin^{-/-}$ T cells exhibit enhanced cytokine secretion in young mice before the onset of tissue inflammation or damage. Enhanced cytokine secretion also correlates with inflammation in several mouse models, including the mouse model of oxazolone-induced colitis (7) and the IL-7 transgenic and IL-10-deficient animals (19, 46). T cells from these animals exhibit a three- to fivefold increase in cytokine production which correlates with exaggerated Th1 or Th2 effector T-cell responses (39). In the case of Sin-deficient mice, although both Th1 and

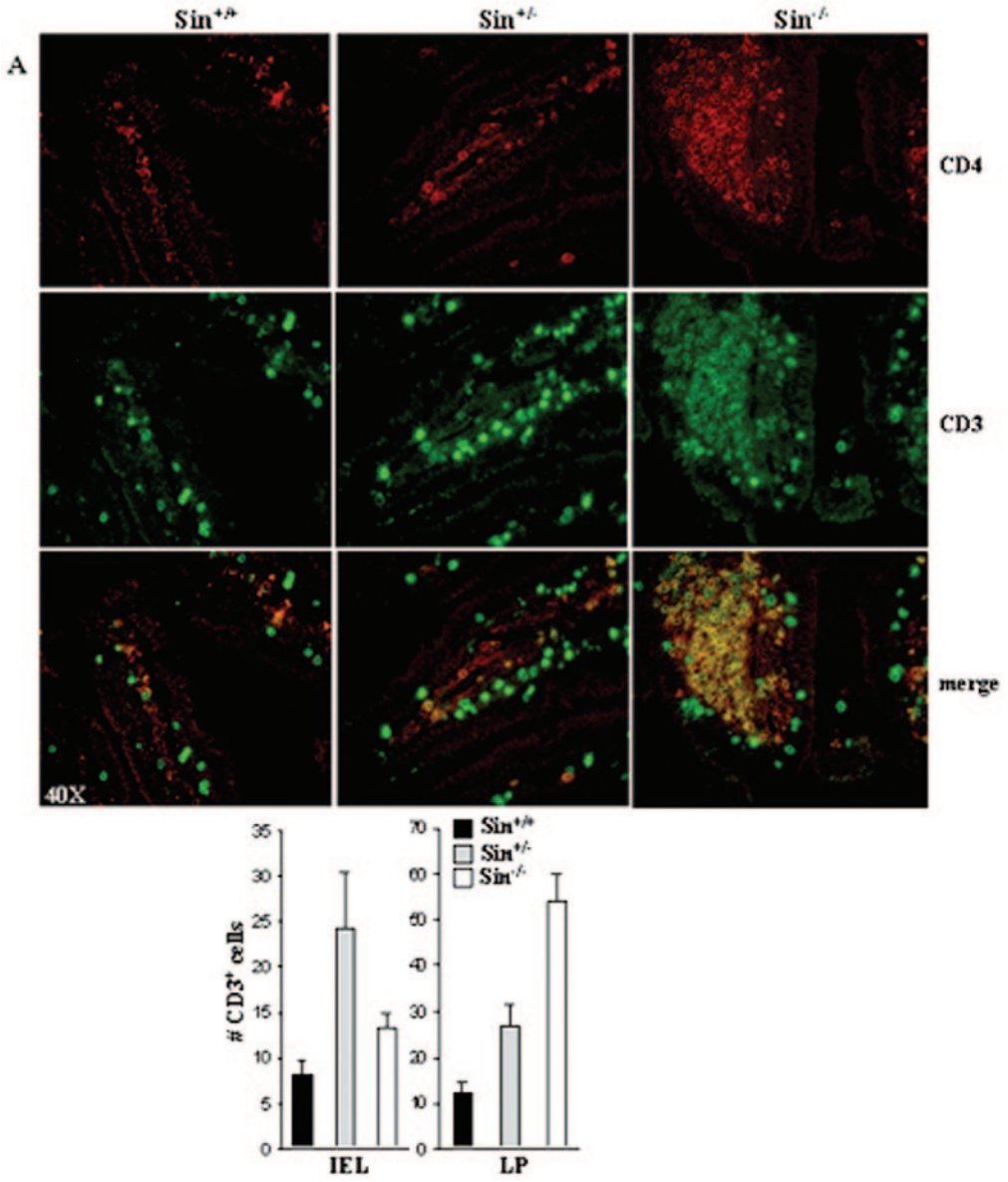

FIG. 5. Increased infiltration by activated $CD4^+$ $CD25^+$ T cells in the laminae propriae of $Sin^{-/-}$ mice. Serial frozen sections of small intestine were costained with anti-CD4- (A) or anti-CD8- (B) and anti-CD3-specific antibodies, and T cells were visualized with anti-rat rhodamine-conjugated (CD4 and CD8) and anti-rabbit AlexaFluor488-conjugated (CD3) secondary antibodies and fluorescent microscopy. Numbers of infiltrating $CD3^+$ intraepithelial (IE) and lamina propria (LP) T cells were determined by counting four random fields of stained villi and represented as means ± standard deviations. Sections from three different mice were used for counting IE and LP $CD3^+$ T cells. (C) Frozen sections from different animals were costained with anti-CD4- and anti-CD25-FITC-specific antibodies and $CD4^+$ $CD25^+$ T cells were visualized with anti-rat rhodamine-conjugated (CD4) secondary antibody and fluorescent microscopy.

Th2 cytokines were produced by $Sin^{-/-}$ T cells in vitro, IL-4/IL-5 production was more pronounced and was accompanied by an in vivo bias towards a Th2 response in the form of significantly increased IgG1 and IgA antibody production after NP-KLH immunization. These observations raise the possibility that inflammation in Sin-deficient mice may be mediated by aberrant Th2 effector T-cell responses; however, the exact nature of the responses and how it compares to other models of mucosal inflammation remain to be determined.

The conclusion that activated $CD4^+$ T cells and increased cytokine production are responsible for the inflammation observed in $Sin^{-/-}$ mice is further supported by studies demonstrating that in vivo activation of T cells through anti-CD3 antibody injection into mice can lead to destruction of the villi in the small intestine (26, 29). Moreover, mice injected with various cytokines, such as IL-12, IFN-γ, and TNF develop severe damage of the intestinal epithelium (14). Again, these effects are similar to those observed in $Sin^{-/-}$ mice and support a role for exaggerated T-cell and cytokine responses in the development of inflammation in these mice.

Given the enhanced T-cell responses of Sin knockout animals, how does Sin deficiency induce spontaneous enteropathy

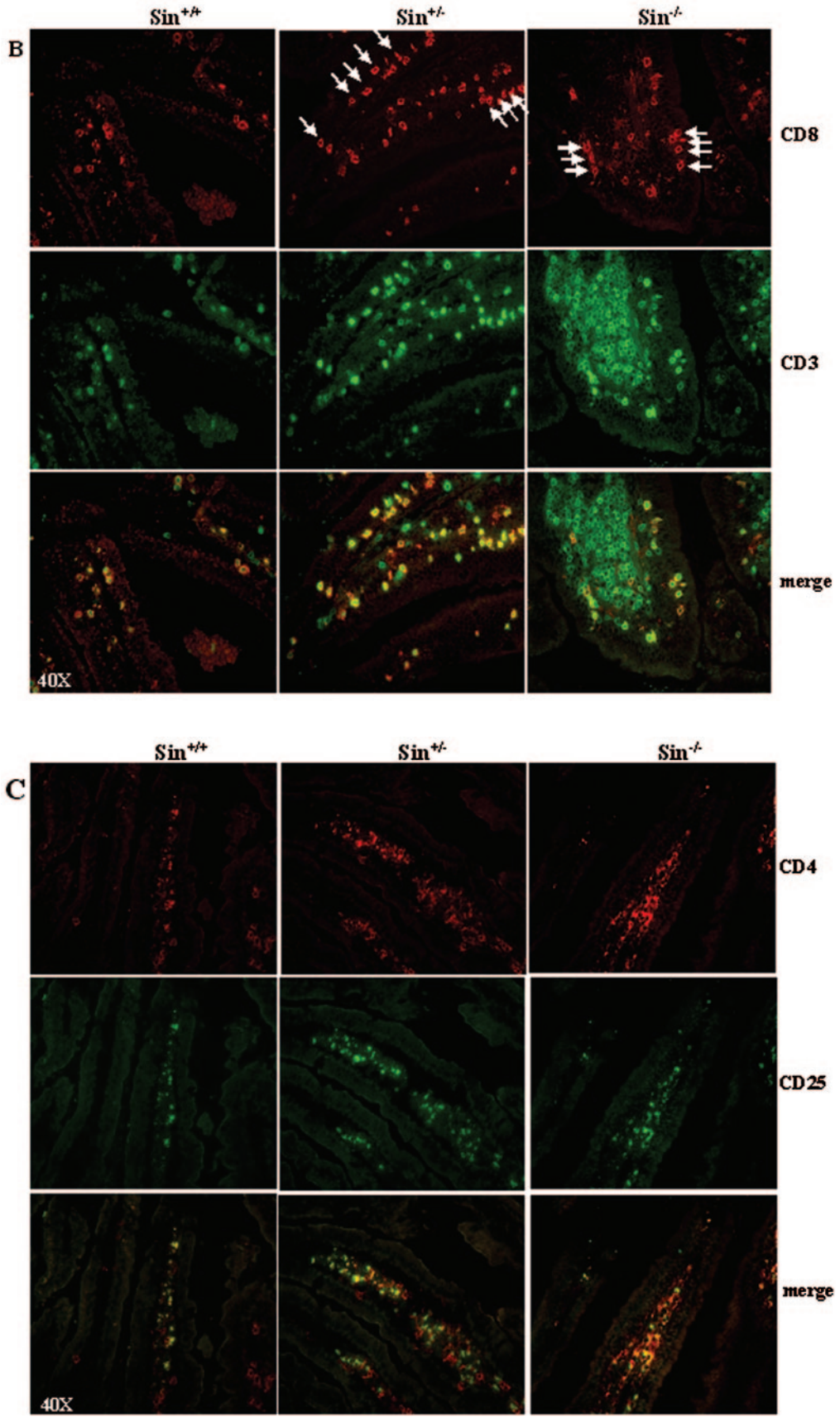

FIG. 5—*Continued.*

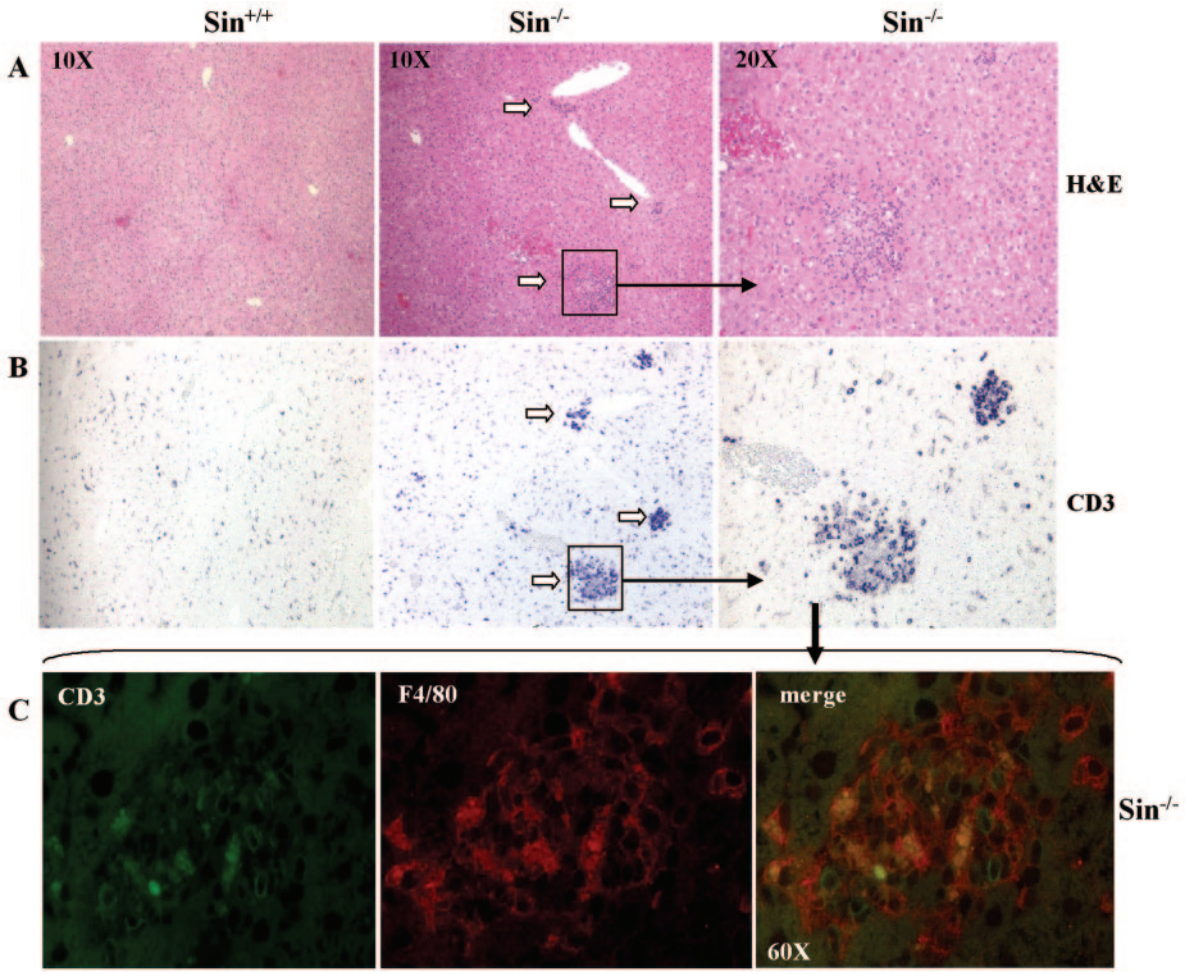

FIG. 6. Presence of inflammatory infiltrates containing $CD3^+$ T cells and macrophages in the livers of aged Sin knockout mice. (A) Paraffin-embedded sections of liver tissue from wild-type and $Sin^{-/-}$ mice were stained with H&E, and slides were visualized by light microscopy. White arrows point to inflammatory infiltrates in the livers of $Sin^{-/-}$ mice. Magnifications (×10) of the livers of wild-type and knockout mice are shown in the left and middle panels, with an enlarged liver section of the knockout (×40) shown on the left. (B) Paraffin-embedded serial sections from the same tissue used as described for panel A were stained with anti-CD3 antibody to reveal the presence of $CD3^+$ T cells. (C) A serial section from the same $Sin^{-/-}$ tissue used in panels A and B (right panels) was costained with F4/80 and anti-CD3 antibodies to reveal the presence of macrophages and T cells in the granulomas and visualized by fluorescent microscopy.

and tissue-specific inflammation? It is well known that the mucosal surface of the gut is constantly exposed to high concentrations of antigens derived from food and microorganisms, leading to continuous stimulation of the intestinal immune system. Although the presence of these antigens is tolerated under normal conditions, disturbances in the function of the immune system lead to aberrant responses against these antigens and development of inflammation. Disturbances in the function of the immune system leading to mucosal inflammation can be caused by excessive effector or defective regulatory T-cell (T_{reg}) function. For example, whereas the majority of mouse models exhibit excessive effector responses, the IL-10 knockout mice develop colitis as a result of defective function of T_{reg} due to lack of suppressive function by IL-10 (19, 46). In the case of the Sin knockout mice, the presence of infiltrating $CD4^+$ $CD25^+$ T cells in the laminae propriae of $Sin^{-/-}$ mice and the normal percentages of $CD4^+$ $CD25^+$ T cells suggest that inflammation in these mice is likely due to chronically enhanced effector responses by activated $CD4^+$ T cells rather than defective suppressor function by T_{reg}. However, in the absence of direct evidence that the suppressor function of $Sin^{-/-}$ $CD4^+$ T cells is intact, we currently cannot exclude the possibility that the T_{reg} responses of Sin deficient mice are compromised.

TABLE 3. Presence of inflammation in tissues of Sin-deficient mice[a]

Mouse type	No. of mice with inflammation in indicated type of tissue/total no. of mice			
	Liver	Kidney	Lung	Skin
$Sin^{+/+}$	0/7	1/6	1/6	0/6
$Sin^{+/-}$	1/7	2/6	1/6	2/6
$Sin^{-/-}$	5/7	4/6	3/6	2/6

[a] Presence of inflammatory infiltrates was determined by analyzing H&E-stained paraffin sections of different tissues under a light microscope and by staining sections with anti-CD3 antibody.

In addition to perturbations in effector and/or T_{reg} functions, $CD8^+$ T-cell-mediated cytotoxicity has been implicated as a driving factor in the development of colitis in at least one other experimental model, the $TNF^{\Delta ARE}$ mice mentioned above (18). Thus, the increased presence of cytotoxic $CD8^+$ cells in the intestinal epithelia of $Sin^{+/-}$ and $Sin^{-/-}$ mice may lead to cytotoxic elimination of the intestinal epithelium, increased exposure of lymphoid cells to luminal antigens, and exacerbation of the inflammatory response. On the other hand, growing evidence suggests that $CD8^+$ T cells are immunoregulatory and can protect host tissues from uncontrolled infiltration by systemic cells (15). Whether this is the case in $Sin^{+/-}$ mice, which as a whole exhibit an increased presence of $CD8^+$ T cells and a milder form of the disease, is unclear. Our future experiments will examine the mechanisms through which Sin deficiency results in mucosal inflammation and whether effector and/or suppressor responses are perturbed, as well as the nature of the T-cell subpopulation(s) responsible for disease development in Sin knockout mice.

Finally, the inflammation evident in Sin-deficient mice differs from that observed in other mouse models of mucosal inflammation in that $Sin^{-/-}$ mice do not develop colitis. However, a histopathology similar to that of $Sin^{-/-}$ mice is observed in the SAMP/Yit animals which develop spontaneous and chronic ileitis with resemblance to human Crohn's disease (25). Similar to our Sin-deficient animals, the histopathology of mucosal inflammation in the SAMP/Yit mice is characterized by chronic inflammation, villus infiltration by $CD3^+$ T cells, crypt enlargement, and changes in epithelial cell architecture (25). Interestingly, recent human linkage studies have identified a particular region on chromosome 14, q11.2-12, which correlates with Crohn's disease development and is designated as the inflammatory bowel disease 4 (IBD4) locus (1, 12, 22, 24, 44, 45). The *sin/efs* genomic locus also localizes in region 14q11.2-12 in close proximity to the IBD4 locus, raising the possibility that Sin plays a role in the development of a Crohn's disease-related enteropathy. In conclusion, as an animal model, the Sin knockout mice may contribute to a better understanding of the mechanisms that drive mucosal inflammation and combined with human studies may implicate Sin in the development of human disease.

ACKNOWLEDGMENTS

We thank Alessandra Pernis, Jessica Fanzo, and So Young Jang for technical advice and reagents; Raphael Clynes and Ramon Parsons for providing fluorescent microscopes; Kevan Herold and Qiong-Fen Guo for assistance with the cytokine assays; and Mathias Szabolcs for evaluating histology sections.

This work was supported in part by the American Cancer Society grant RPG99-09-01MGO, by the Department of Defense grants DAMD17-99-1-9151 and DAMD17-99-1-915, and by the National Institute of Allergy and Infectious Disease grant RO1 AI49387-01.

REFERENCES

1. **Ahmad, T., J. Satsangi, D. McGovern, M. Bunce, and D. P. Jewell.** 2001. Review article: the genetics of inflammatory bowel disease. Aliment. Pharmacol. Ther. **15:**731–748.
2. **Alexandropoulos, K., and D. Baltimore.** 1996. Coordinate activation of c-Src by SH3- and SH2-binding sites on a novel p130Cas-related protein, Sin. Genes Dev. **10:**1341–1355.
3. **Alexandropoulos, K., L. T. Donlin, L. Xing, and A. G. Regelmann.** 2003. Sin: good or bad? A T lymphocyte perspective. Immunol. Rev. **192:**181–195.
4. **Azzam, H. S., A. Grinberg, K. Lui, H. Shen, E. W. Shores, and P. E. Love.** 1998. CD5 expression is developmentally regulated by T cell receptor (TCR) signals and TCR avidity. J. Exp. Med. **188:**2301–2311.
5. **Bendelac, A., P. Matzinger, R. A. Seder, W. E. Paul, and R. H. Schwartz.** 1992. Activation events during thymic selection. J. Exp. Med. **175:**731–742.
6. **Blumberg, R. S., L. J. Saubermann, and W. Strober.** 1999. Animal models of mucosal inflammation and their relation to human inflammatory bowel disease. Curr. Opin. Immunol. **11:**648–656.
7. **Boirivant, M., I. J. Fuss, A. Chu, and W. Strober.** 1998. Oxazolone colitis: a murine model of T helper cell type 2 colitis treatable with antibodies to interleukin 4. J. Exp. Med. **188:**1929–1939.
8. **Bouma, G., and W. Strober.** 2003. The immunological and genetic basis of inflammatory bowel disease. Nat. Rev. Immunol. **3:**521–533.
9. **Chiang, Y. J., H. K. Kole, K. Brown, M. Naramura, S. Fukuhara, R. J. Hu, I. K. Jang, J. S. Gutkind, E. Shevach, and H. Gu.** 2000. Cbl-b regulates the CD28 dependence of T-cell activation. Nature **403:**216–220.
10. **Cote, J. F., A. Charest, J. Wagner, and M. L. Tremblay.** 1998. Combination of gene targeting and substrate trapping to identify substrates of protein tyrosine phosphatases using PTP-PEST as a model. Biochemistry **37:**13128–13137.
11. **Donlin, L. T., C. A. Roman, M. Adlam, A. G. Regelmann, and K. Alexandropoulos.** 2002. Defective thymocyte maturation by transgenic expression of a truncated form of the T lymphocyte adapter molecule and Fyn substrate, Sin. J. Immunol. **169:**6900–6909.
12. **Duerr, R. H., M. M. Barmada, L. Zhang, R. Pfutzer, and D. E. Weeks.** 2000. High-density genome scan in Crohn disease shows confirmed linkage to chromosome 14q11-12. Am. J. Hum. Genet. **66:**1857–1862.
13. **Green, P. H., and B. Jabri.** 2003. Coeliac disease. Lancet **362:**383–391.
14. **Guy-Grand, D., J. P. DiSanto, P. Henchoz, M. Malassis-Seris, and P. Vassalli.** 1998. Small bowel enteropathy: role of intraepithelial lymphocytes and of cytokines (IL-12, IFN-gamma, TNF) in the induction of epithelial cell death and renewal. Eur. J. Immunol. **28:**730–744.
15. **Hayday, A., E. Theodoridis, E. Ramsburg, and J. Shires.** 2001. Intraepithelial lymphocytes: exploring the Third Way in immunology. Nat. Immunol. **2:**997–1003.
16. **Hibi, T., H. Ogata, and A. Sakuraba.** 2002. Animal models of inflammatory bowel disease. J. Gastroenterol. **37:**409–417.
17. **Kishihara, K., J. Penninger, V. A. Wallace, T. M. Kundig, K. Kawai, A. Wakeham, E. Timms, K. Pfeffer, P. S. Ohashi, M. L. Thomas, et al.** 1993. Normal B lymphocyte development but impaired T cell maturation in CD45-exon6 protein tyrosine phosphatase-deficient mice. Cell **74:**143–156.
18. **Kontoyiannis, D., G. Boulougouris, M. Manoloukos, M. Armaka, M. Apostolaki, T. Pizarro, A. Kotlyarov, I. Forster, R. Flavell, M. Gaestel, P. Tsichlis, F. Cominelli, and G. Kollias.** 2002. Genetic dissection of the cellular pathways and signaling mechanisms in modeled tumor necrosis factor-induced Crohn's-like inflammatory bowel disease. J. Exp. Med. **196:**1563–1574.
19. **Kuhn, R., J. Lohler, D. Rennick, K. Rajewsky, and W. Muller.** 1993. Interleukin-10-deficient mice develop chronic enterocolitis. Cell **75:**263–274.
20. **Law, S. F., Y. Z. Zhang, S. J. Fashena, G. Toby, J. Estojak, and E. A. Golemis.** 1999. Dimerization of the docking/adaptor protein HEF1 via a carboxy-terminal helix-loop-helix domain. Exp. Cell Res. **252:**224–235.
21. **Lefkowitch, J. H.** 1999. Hepatic granulomas. J. Hepatol. **30**(Suppl. 1)**:**40–45.
22. **Ma, Y., J. D. Ohmen, Z. Li, L. G. Bentley, C. McElree, S. Pressman, S. R. Targan, N. Fischel-Ghodsian, J. I. Rotter, and H. Yang.** 1999. A genome-wide search identifies potential new susceptibility loci for Crohn's disease. Inflamm. Bowel Dis. **5:**271–278.
23. **Majeti, R., Z. Xu, T. G. Parslow, J. L. Olson, D. I. Daikh, N. Killeen, and A. Weiss.** 2000. An inactivating point mutation in the inhibitory wedge of CD45 causes lymphoproliferation and autoimmunity. Cell **103:**1059–1070.
24. **Mathew, C. G., and C. M. Lewis.** 2004. Genetics of inflammatory bowel disease: progress and prospects. Hum. Mol. Genet. **13:**R161–R168.
25. **Matsumoto, S., Y. Okabe, H. Setoyama, K. Takayama, J. Ohtsuka, H. Funahashi, A. Imaoka, Y. Okada, and Y. Umesaki.** 1998. Inflammatory bowel disease-like enteritis and caecitis in a senescence accelerated mouse P1/Yit strain. Gut **43:**71–78.
26. **Merger, M., J. L. Viney, R. Borojevic, D. Steele-Norwood, P. Zhou, D. A. Clark, R. Riddell, R. Maric, E. R. Podack, and K. Croitoru.** 2002. Defining the roles of perforin, Fas/FasL, and tumour necrosis factor alpha in T cell induced mucosal damage in the mouse intestine. Gut **51:**155–163.
27. **Morrissey, P. J., K. Charrier, S. Braddy, D. Liggitt, and J. D. Watson.** 1993. CD4+ T cells that express high levels of CD45RB induce wasting disease when transferred into congenic severe combined immunodeficient mice. Disease development is prevented by cotransfer of purified CD4+ T cells. J. Exp. Med. **178:**237–244.
28. **Murphy, M. A., R. G. Schnall, D. J. Venter, L. Barnett, I. Bertoncello, C. B. Thien, W. Y. Langdon, and D. D. Bowtell.** 1998. Tissue hyperplasia and enhanced T-cell signalling via ZAP-70 in c-Cbl-deficient mice. Mol. Cell. Biol. **18:**4872–4882.
29. **Musch, M. W., L. L. Clarke, D. Mamah, L. R. Gawenis, Z. Zhang, W. Ellsworth, D. Shalowitz, N. Mittal, P. Efthimiou, Z. Alnadjim, S. D. Hurst, E. B. Chang, and T. A. Barrett.** 2002. T cell activation causes diarrhea by increasing intestinal permeability and inhibiting epithelial Na+/K+-ATPase. J. Clin. Investig. **110:**1739–1747.

30. **Naramura, M., H. K. Kole, R. J. Hu, and H. Gu.** 1998. Altered thymic positive selection and intracellular signals in Cbl-deficient mice. Proc. Natl. Acad. Sci. USA **95:**15547–15552.
31. **O'Neill, G. M., S. J. Fashena, and E. A. Golemis.** 2000. Integrin signalling: a new Cas(t) of characters enters the stage. Trends Cell Biol. **10:**111–119.
32. **Pizarro, T. T., K. O. Arseneau, G. Bamias, and F. Cominelli.** 2003. Mouse models for the study of Crohn's disease. Trends Mol. Med. **9:**218–222.
33. **Powrie, F., M. W. Leach, S. Mauze, L. B. Caddle, and R. L. Coffman.** 1993. Phenotypically distinct subsets of CD4+ T cells induce or protect from chronic intestinal inflammation in C. B-17 scid mice. Int. Immunol. **5:**1461–1471.
34. **Simpson, S. J., E. Mizoguchi, D. Allen, A. K. Bhan, and C. Terhorst.** 1995. Evidence that CD4+, but not CD8+ T cells are responsible for murine interleukin-2-deficient colitis. Eur. J. Immunol. **25:**2618–2625.
35. **Sollid, L. M.** 2002. Coeliac disease: dissecting a complex inflammatory disorder. Nat. Rev. Immunol. **2:**647–655.
36. **Songyang, Z., S. E. Shoelson, M. Chaudhuri, G. Gish, T. Pawson, W. G. Haser, F. King, T. Roberts, S. Ratnofsky, R. J. Lechleider, et al.** 1993. SH2 domains recognize specific phosphopeptide sequences. Cell **72:**767–778.
37. **Sosinowski, T., N. Killeen, and A. Weiss.** 2001. The Src-like adaptor protein downregulates the T cell receptor on CD4+CD8+ thymocytes and regulates positive selection. Immunity **15:**457–466.
38. **Stavnezer, J.** 1996. Immunoglobulin class switching. Curr. Opin. Immunol. **8:**199–205.
39. **Strober, W., I. J. Fuss, and R. S. Blumberg.** 2002. The immunology of mucosal models of inflammation. Annu. Rev. Immunol. **20:**495–549.
40. **Strober, W., I. J. Fuss, R. O. Ehrhardt, M. Neurath, M. Boirivant, and B. R. Ludviksson.** 1998. Mucosal immunoregulation and inflammatory bowel disease: new insights from murine models of inflammation. Scand. J. Immunol. **48:**453–458.
41. **Stuber, E., and W. Strober.** 1996. The T cell-B cell interaction via OX40-OX40L is necessary for the T cell-dependent humoral immune response. J. Exp. Med. **183:**979–989.
42. **Tivol, E. A., F. Borriello, A. N. Schweitzer, W. P. Lynch, J. A. Bluestone, and A. H. Sharpe.** 1995. Loss of CTLA-4 leads to massive lymphoproliferation and fatal multiorgan tissue destruction, revealing a critical negative regulatory role of CTLA-4. Immunity **3:**541–547.
43. **Tseveleki, V., J. Bauer, E. Taoufik, C. Ruan, L. Leondiadis, S. Haralambous, H. Lassmann, and L. Probert.** 2004. Cellular FLIP (long isoform) overexpression in T cells drives Th2 effector responses and promotes immunoregulation in experimental autoimmune encephalomyelitis. J. Immunol. **173:**6619–6626.
44. **van Heel, D. A., S. A. Fisher, A. Kirby, M. J. Daly, J. D. Rioux, and C. M. Lewis.** 2004. Inflammatory bowel disease susceptibility loci defined by genome scan meta-analysis of 1952 affected relative pairs. Hum. Mol. Genet. **13:**763–770.
45. **Vermeire, S., P. Rutgeerts, K. Van Steen, S. Joossens, G. Claessens, M. Pierik, M. Peeters, and R. Vlietinck.** 2004. Genome wide scan in a Flemish inflammatory bowel disease population: support for the IBD4 locus, population heterogeneity, and epistasis. Gut **53:**980–986.
46. **Watanabe, M., Y. Ueno, T. Yajima, S. Okamoto, T. Hayashi, M. Yamazaki, Y. Iwao, H. Ishii, S. Habu, M. Uehira, H. Nishimoto, H. Ishikawa, J. Hata, and T. Hibi.** 1998. Interleukin 7 transgenic mice develop chronic colitis with decreased interleukin 7 protein accumulation in the colonic mucosa. J. Exp. Med. **187:**389–402.
47. **Waterhouse, P., J. M. Penninger, E. Timms, A. Wakeham, A. Shahinian, K. P. Lee, C. B. Thompson, H. Griesser, and T. W. Mak.** 1995. Lymphoproliferative disorders with early lethality in mice deficient in Ctla-4. Science **270:**985–988.
48. **Wirtz, S., and M. F. Neurath.** 2000. Animal models of intestinal inflammation: new insights into the molecular pathogenesis and immunotherapy of inflammatory bowel disease. Int. J. Colorectal Dis. **15:**144–160.
49. **Xing, L., L. T. Donlin, R. H. Miller, and K. Alexandropoulos.** 2004. The adapter molecule Sin regulates T-cell-receptor-mediated signal transduction by modulating signaling substrate availability. Mol. Cell. Biol. **24:**4581–4592.